Annual Top 10 Science Advances of 2021 in China
— Glory moments flash back

By SONG Jianlan and YAN Fusheng (Staff Reporters)

China's Mars probe, *Tianwen*-1's successful soft landing on the surface of the Red Planet, ranked first in China's "Annual Top 10 Science Advances" of 2021, as announced by the High Technology Research and Development Center (HTRDC) of the Chinese Ministry of Science and Technology on February 28, 2022. Several other space missions, including the successful launch of *Tianhe* — the core module of China's space station, the successful flights of *Shenzhou*-12 and *Shenzhou*-13 manned spaceships and their successful dockings onto *Tianhe*, and the first results from the analysis of lunar samples returned by *Chang'e*-5, also ranked high in the list, highlighting a bumper year for aerospace advances of China.

This, however, did not overshadow other scintillating feats, particularly the first successful effort to artificially synthesize starch from carbon dioxide without aid from biological cell or chloroplast – a long dream come true that might help human beings with food security and the global warming issue, the capture by FAST of the biggest sample of burst events from a repeating fast radio burst (FRB), and the discovery of underlying mechanism of SARS-CoV-2's escape from anti-virus drugs.

This marks the 17th election and release of the top-10 list, which aims to promote science advancement and increase the public awareness of science.

Now, let's embark on the journey back to the glory moments of 2021.

Tianwen-1, the first Mars probe of China (Image: HTRDC)

1st Successful Landing of *Tianwen*-1 on Mars Surface

At 7:18 on the morning of May 15, 2021, the lander of *Tianwen*-1, the first Mars Probe of China, softly touches down on the *Utopia Planitia*, its preset landing site on the Martian surface, marking the success of China's first attempt to land on the Red Planet. The mission adopted a four-step cascade decelerating strategy to secure the safe touchdown, integrating aerodynamic braking, parachute decelerating, motor deceleration and soft-landing buffer. The probe demonstrated an excellent ability to deal with the extreme conditions and complicated local environments, as the result from an optimized R&D process and methodology.

The touch-down by the lander of *Tianwen*-1 marks the first successful effort of China to land on an exoplanet. Launched on July 23, 2020, *Tianwen*-1 mission is designed to investigate the Red Planet's morphology and geological structure, its surface soil characteristics as well as water-ice distribution, its surface material composition, atmospheric ionized layer, climate and environment, and its physical fields and inner structures. As an initiator of China's Mars Exploration Program, the Chinese Academy of Sciences (CAS) has been seeing through the Program's implementation.

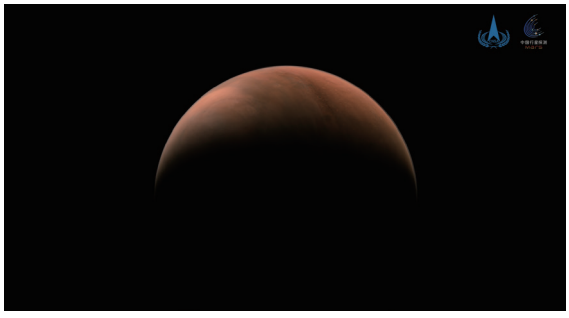

The profile of Mars shot by *Tianwen*-1, the Mars probe of China from the northern celestial hemisphere, as released by the China National Space Administration (CNSA) on March 26, 2021, when the probe was still heading to the Red Planet. (Image: CNSA)

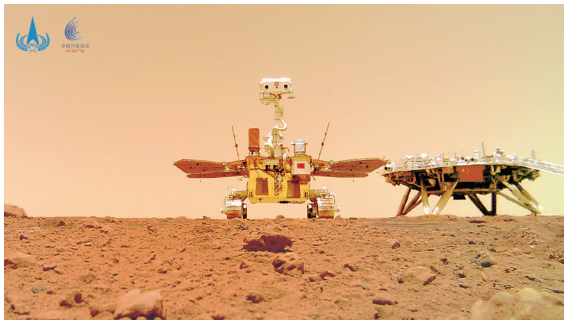

Zhurong (left), the Chinese Mars rover named after the Chinese God of Fire, poses together with the lander on the Red Planet. One week after its successful soft landing, the lander of *Tianwen*-1 released the 240-kg rover to conduct *in situ* investigations across the Martian terrains. (Image: CNSA/MARS)

2nd The Successful Launch of *Tianhe* and the Subsequent Successful Flights and Dockings of *Shenzhou*-12 and *Shenzhou*-13 onto the Core Module

On April 29, 2021, *Tianhe*, the core module of China's space station, was accurately sent into its preset orbit from the Wenchang Aerospace Launching Site in Hainan province of China. This also sent the construction of China's space station into a new stage, laying a solid foundation for the

Illustration of China's space station. (Image: CNSA)

ensuing missions. Later on June 17, *Shenzhou*-12 flew into space and successfully docked onto the core module, sending three astronauts, namely NIE Haisheng, LIU Boming and TANG Hongbo into space. This was for the first time a manned spaceship docked onto the core module since the latter's in-orbit operation, and unveiled the era of space station for China, in which manned spaceships began to shuttle to and from the space station as a routine. Further, the day October 16 saw the successful flight of *Shenzhou*-13 and its active, rapid docking onto *Tianhe*, sending three more astronauts, ZHAI Zhigang, WANG Yaping and YE Guangfu into orbit. This marks another milestone in China's space exploration: the first success in radial docking between spacecraft in orbit.

3rd The Cell-free *de novo* Synthesis of Starch from Carbon Dioxide

The synthesis of starch, the primary component of grains and also an important industrial raw material, has been the exclusive privilege of the biological universe, particularly plants. How the tiny chloroplast manages to harvest and fix the energy from sunlight into this caloric chemical, a compound of water and carbon dioxide (CO_2), has fascinated scientists for long. The light harvesting technique of plants is fabulous, so is their capacity of utilizing – and fixing – carbon dioxide. It would be a dual trophy if only human beings could reduce this greenhouse gas from the atmosphere and meanwhile synthesize starch from it.

Now Chinese scientists have made this dream come true.

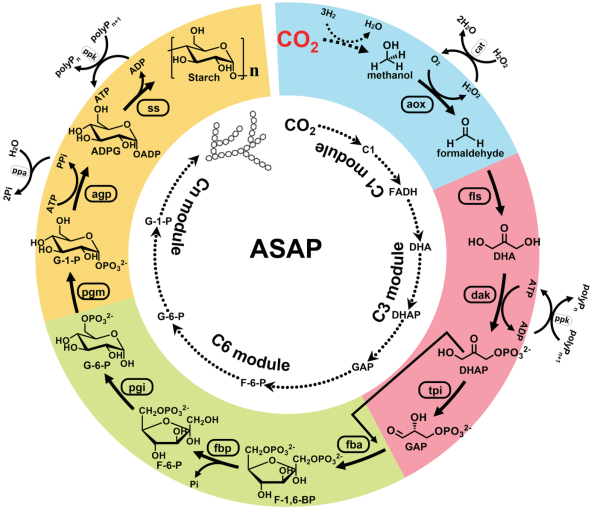

Design and modular assembly of the artificial starch anabolic pathway. (Image by CAS)

On September 24, a team of scientists led by Prof. MA Yanhe at the Tianjin Institute of Industrial Biotechnology (TIB), CAS reported in *Science* the first successful cell-free *de novo* synthesis of starches (amylose and amylopectin). The team successfully converted CO_2 to starch at a rate about 8.5 times faster than natural synthesis in maize, driven by hydrogen via a network of 11 core reactions called artificial starch anabolic pathway (ASAP) designed and developed by them. This is a chemical-biochemical hybrid pathway for starch synthesis from CO_2 and hydrogen in a cell-free system. For the first time, human beings do not need to rely on photosynthesis in nature to produce this carbohydrate, offering a new way towards food security and, carbon fixation.

The ASAP network was drafted by computational pathway design, established through modular assembly and substitution, and optimized by protein engineering of three bottleneck-associated enzymes. It is able to convert CO_2 to starch at a rate of 22 nanomoles of CO_2 per minute per milligram of total catalyst, an ~8.5-fold higher rate than starch synthesis in maize. Theoretically, this method can transform energy at an efficiency rate of 7%, about 3.5 folds of those in corps represented by maize. Also it can achieve controlled synthesis of either amylose or amylopectin, opening a new way toward future chemo-biohybrid starch synthesis from CO_2.

Reference

Cai, T., Sun, H., and Qiao, J. *et al*. Cell-free chemoenzymatic starch synthesis from carbon dioxide. *Science* **373**, 1523–1527 (2021). DOI: 10.1126/science.abh4049

4th Lunar Samples Returned by *Chang'e*-5 Reveal Secrets of the Moon's Evolution

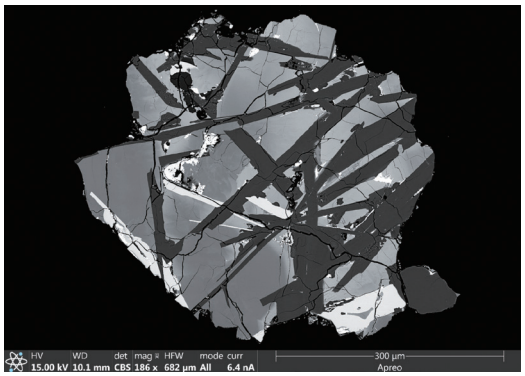

Microscopic image of the lunar sample returned by *Chang'e*-5 (Image by CAS)

Based on their built-up in dating techniques of ultra-high spatial resolution and isotopic analysis, a joint team of scientists from two CAS institutions conducted accurate chronologic, lithogeochemistric research and assay of the samples' magmatic water content. The researchers, represented by Profs. LI Xianhua, YANG Wei, HU Sen and LIN Yangting from the Institute of Geology and Geophysics, CAS and Prof. LI Chunlai from the National Astronomical Observatories, CAS, demonstrated that the lunar basalt sample returned by *Chang'e*-5 formed about 2.30±0.04 billion years ago, and confirmed that the lunar volcanic activity continued until about 2 billion years ago – 800 million years longer than previously constrained by analysis of past lunar samples. This result provided an important "anchor point" for the dating of impact craters, significantly improving the dating accuracy of such impact craters on planetary surfaces in the solar system. Their research also revealed that the lunar mantle yielding the sample is not rich in radioactive heat production elements or water, hence ruling out the chances of two hypothetic melting mechanisms for lunar mantle: the meltdown is neither due to the heat generated by radioactive elements nor lowered melting point by water.

References

Li, QL., Zhou, Q. and Liu, Y. *et al*. Two-billion-year-old volcanism on the Moon from *Chang'e*-5 basalts. *Nature* **600**, 54–58 (2021). https://doi.org/10.1038/s41586-021-04100-2

Tian, HC., Wang, H. and Chen, Y. *et al*. Non-KREEP origin for *Chang'e*-5 basalts in the Procellarum KREEP Terrane. *Nature* **600**, 59–63 (2021). https://doi.org/10.1038/s41586-021-04119-5

Hu, S., He, H. and Ji, J. *et al*. A dry lunar mantle reservoir for young mare basalts of *Chang'e*-5. *Nature* **600**, 49–53 (2021). https://doi.org/10.1038/s41586-021-04107-9

Li, C., Hu, H., and Yang, M.F., *et al*. Characteristics of the lunar samples returned by the *Chang'e*-5 mission. *National Science Review* **9**: nwab188 (2022). https://doi.org/10.1093/nsr/nwab188

5th How SARS-CoV-2 Dodges the Bullet

The pandemic of coronavirus disease 2019 (COVID-19), caused by severe acute respiratory syndrome coronavirus 2 (SARS-CoV-2), has been pushing worldwide public health and economies to the verge of collapse. Over the past two years, we have seen the variants of SARS-CoV-2 popping up continuously, Alpha, Beta, Gamma, Delta, and Omicron…, and it seems that the Greek alphabets won't hold up long before being used up. Ironically, unlike most RNA viruses, CoVs deploy a special duty post to proofread the incorporated ribonucleotides to erase mutations. Accidentally, this proofreader also happens to remove a certain kind of antiviral drugs, namely nucleoside analogs (NAs), which exert their effect by incorporating into viral genomes and subsequently disrupting viral replication and fidelity. As a result, this proofreader helps CoVs dodging these antiviral bullets.

Previous studies pin down this proofreading culprit as a molecular machinery called replication-transcription

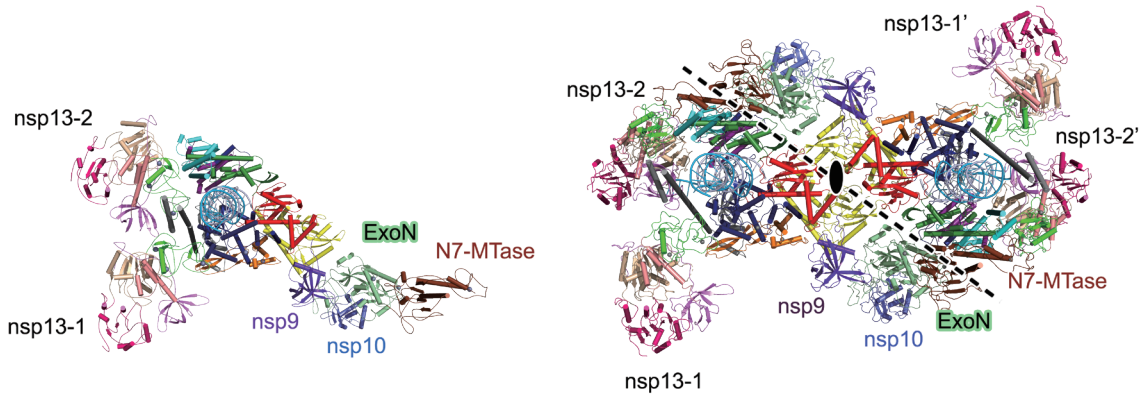

The architecture of RTC in both monomeric (A) and dimeric (B) forms. (Image by YAN *et al.*, 2021)

complex, or RTC, an assembly of many nonstructural proteins that do not presented in the virions. However, the structural details as to how its core components come together and work together remain elusive.

To dissect these mechanisms, a joint team led by LOU Zhiyong and RAO Zihe from Tsinghua University, and GAO Yan from ShanghaiTech University, identified the RTC in a form as Cap(0)-RTC and illustrated the cryoelectron microscopy (cryo-EM) structure of Cap(0)-RTC in both monomeric and dimeric forms to 3.78 Å and 3.35 Å.

The study was appeared in *Cell* in June 2021, entitled "Coupling of N7-methyltransferase and 3'-5' exoribonuclease with SARS-CoV-2 polymerase reveals mechanisms for capping and proofreading".

"The structure not only reveals the architecture of the capping machinery coupled to RTC that achieves the capping actions decorating the 5' end of pre-mRNA but also provides a structural basis to understand the polymerase activity and the mechanism by which nsp14 ExoN is used for proofreading," wrote the authors in the article.

By scrutinizing the monomeric Cap(0)-RTC structure, they found that the catalytic center of exoribonuclease is distal from the polymerase reaction center, indicating the chance of proofreading occurring in the monomeric Cap(0)-RTC is very low.

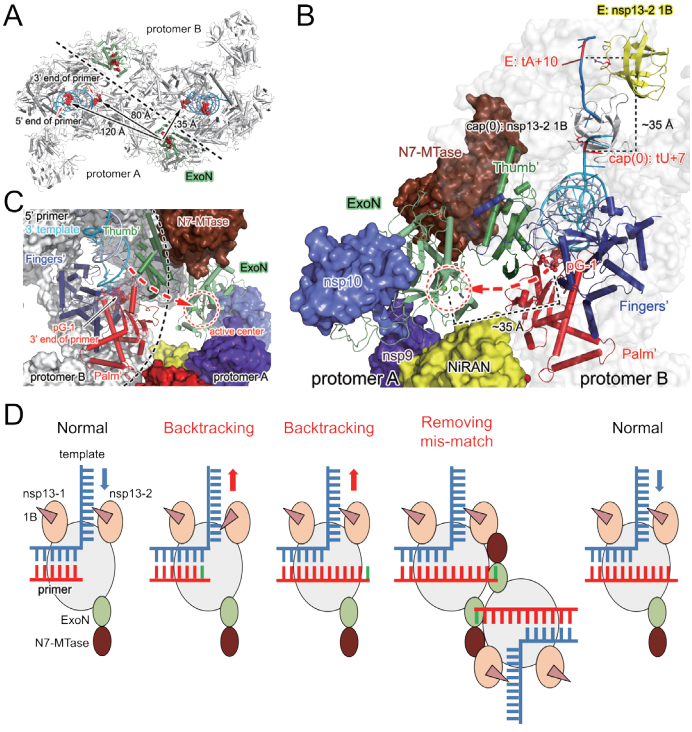

The dimeric Cap(0)-RTC indicated with distances between different functional parts (A) and a close-up view of the machinery (B, C) with proposed model of *in trans* backtracking proofreading (D). The nsp14 ExoN (green) from one Cap(0)-RTC facilitates proofreading of the RNA in concert with polymerase nsp12 (gray) from the other Cap(0)-RTC. The blue and red bars represent the correct nucleotides in template and primer RNAs, while the green bars indicate the mismatched nucleotides. (Image by YAN *et al.*, 2021)

When looking into a dimeric form of Cap(0)-RTC, they found that the polymerase reaction center in one Cap(0)-RTC protomer is ~35 Å away from the catalytic center of exoribonuclease in another Cap(0)-RTC protomer. Backtracking of six-nucleotide RNA could eliminate this short distance. Based on these structure features, they proposed an *in trans* backtracking mechanism for SARS-CoV-2 proofreading that enables specific excision of mismatched nucleotide – In the dimeric form, nsp14 ExoN from one Cap(0)-RTC facilitates proofreading of the RNA

in concert with polymerase nsp12 from the other Cap(0)-RTC.

The unique proofreading mechanism also explains the reduced inhibitory efficacy of nucleotide analog inhibitors, such as remdesivir. Meanwhile, this is also why EIDD-1931, another nucleotide analog that cannot be recognized and excised by Cap(0)-RTC, shows enhanced efficacy against SARS-CoV-2 containing resistance mutations to remdesivir.

In *Spiderman*, "with great power comes great responsibility"; for molecules in biology, with great responsibility comes great conservation, *i.e.*, little room for changes. Hence, Cap(0)-RTC represents a core target for broad-spectrum antiviral drugs against CoVs.

Reference

Yan, L., Yang, Y., and Li, M., *et al*. Coupling of N7-methyltransferase and 3′-5′ exoribonuclease with SARS-CoV-2 polymerase reveals mechanisms for capping and proofreading. *Cell* 184, 3474 (2021). doi: 10.1016/j.cell.2021.05.033.

6th FAST Captured the World's Largest Sample of Fast Radio Burst Events

Fast radio bursts (FRBs) represent the brightest blast in radio bands. Among them, FRB 121102 is the first repeating FRB known to human beings. Using FAST, the Five-hundred-meter Aperture Spherical radio Telescope of China, a group of astronomers led by Prof. LI Di from the National Astronomical Observatories, CAS successfully captured an extremely active phase of FRB 121102, in which it bursted as frequently as 122 times an hour at the peak. The team's observation obtained a total of 1,652 bursting signals at high signal-to-noise ratio, constituting the largest sample of burst events recorded so far. This allowed a statistical research of the bursts, and subsequently led to the discovery of some previously unknown characters of this repeating FRB.

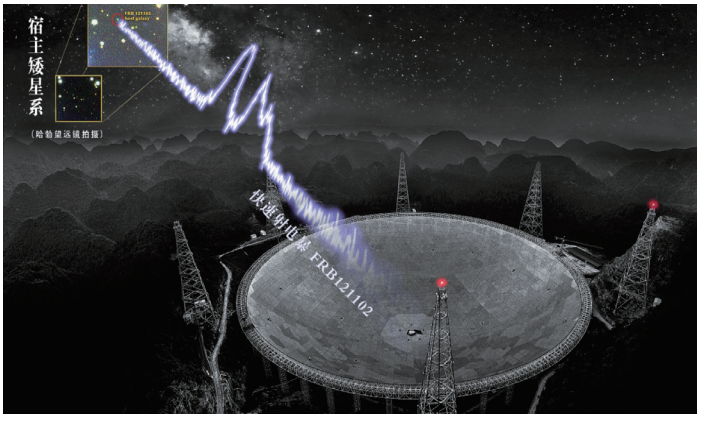

FAST has caught the largest sample of FRB burst events in the world. (Image by CAS)

The research identified the characteristic energy of this FRB's bursting rate as $E_0=4.8\times10^{37}$ erg; also it detected a bimodal distribution of the burst energy. No single functional form can fit this distribution in the full energy range. Rather, at the low-energy end, a log-normal function fits the distribution well, indicating a stochastic process in the bursts. At the high-energy end, a generalized Cauchy function can fit the distribution reasonably well, suggesting a stochastic process dominated by two independent, normally distributed random variables.

Analysis of the sample of burst events ruled out the chances for a period or quasi-period ranging from one microsecond to one hour of this FRB, and strictly constrained the possibility for this repeating FRB to originate from a single compact celestial body.

Reference

Li, D., Wang, P., Zhu, W.W. *et al.* A bimodal burst energy distribution of a repeating fast radio burst source. *Nature* **598**, 267–271 (2021). https://doi.org/10.1038/s41586-021-03878-5

7th Scalable Production of High-performing Fibre Lithium-ion Batteries

Fibre lithium-ion batteries (FLIB) are of significant interest because they can be woven into textiles to power future wearable electronics. However, it is not easy to make long fibre batteries, and longer fibres were thought to have higher internal resistances that could compromise the battery's performance.

Contrary to this very expectation, a team led by PENG Huisheng and CHEN Peining from Fudan University observed an unexpected decrease in internal resistance for the longer fibres. It implies that obtaining high-performing long FLIBs is possible.

Encouraged by this unexpected finding, the team developed a scalable process to produce metres of high-performing FLIBs with an energy density of 85.69 Wh kg^{-1}, which is two orders of magnitude higher than a typical laboratory-scale fibre battery (<1 Wh kg^{-1}). The related work was published in *Nature*.

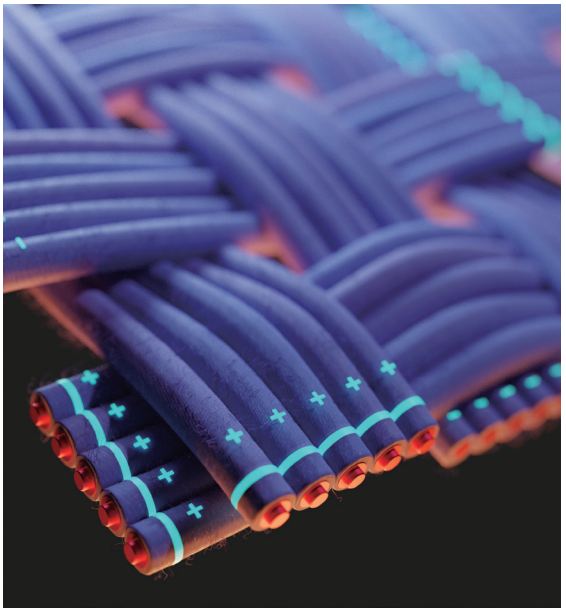

Schematic diagram of the integrated assembly of fibre lithium-ion batteries. (Image by PENG Huisheng and CHEN Peining)

They also established the first industrial-scale fabrication line of FLIBs in the world. The produced FLIBs were highly reproducible and robust, showing similar performance to commercial lithium-ion batteries during the charge-discharge test and working test under low temperatures. These FLIBs are flexible and durable, and can maintain an 80% capacity even after bending for 100,000 cycles.

After weaving the flexible FLIBs into a jacket, they demonstrated that the FLIB textiles could wirelessly charge a smartphone in the wearer's pocket. They further used the FLIB textile to create a jacket that can use a fibre sensor to read the concentrations of Na^+ and Ca^{2+} in the wearer's sweat and show the data on a textile display. This proof-of-concept demonstration shows a great promise of textile FLIBs for personalized real-time health management.

Months later, the same team reported a new and general solution-extrusion method that can produce continuous fibre batteries in a single step, with remarkable production rates of 250 m h^{-1}.

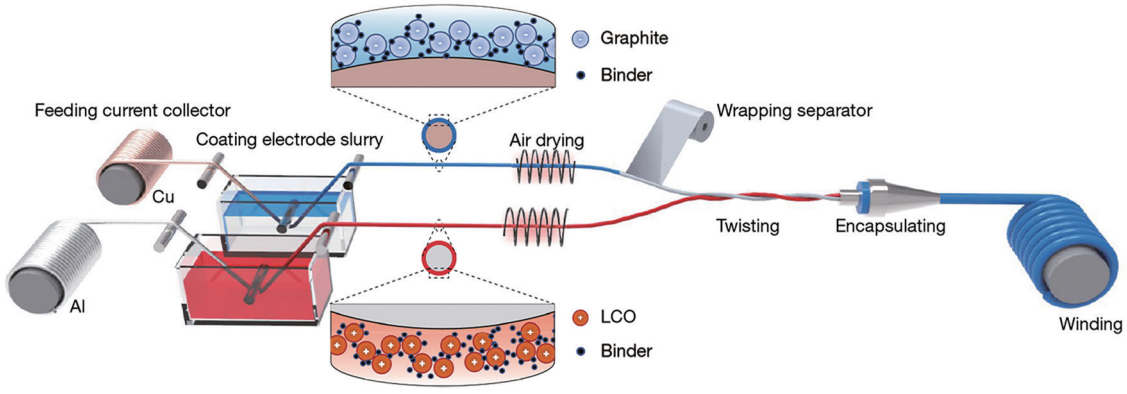

Schematic of the set-up used to produce continuous FLIBs. (Image by HE *et al.*, 2021)

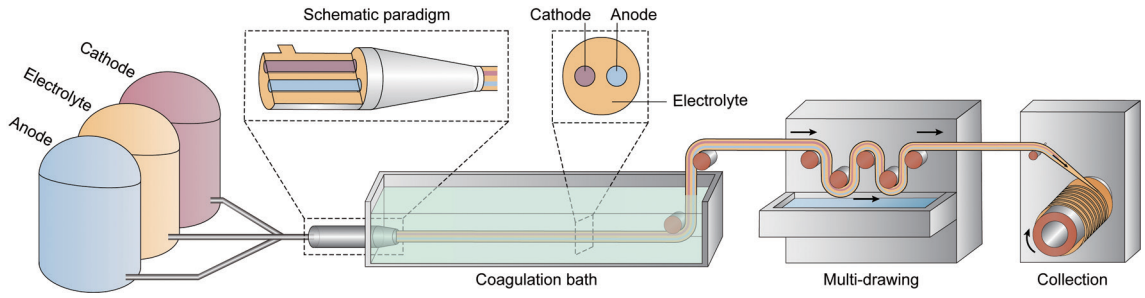

Schematic showing the set-up for producing fibre batteries. (Image by Liao *et al.*, 2022)

This extrusion method starts with preparing cathode, anode and gel electrolyte inks. In a typical run, the inks are simultaneously pumped through separate channels into a tapered spinneret and extruded into a coagulation bath, where the gel electrolyte ink becomes solid quickly around the anode and cathode fibres to form the fibre battery architecture. Subsequently, the extruded fibre batteries are pulled, dried, and collected on a winding spool ready for weaving into textiles.

The researchers did a couple of tricks to ensure the process went smoothly. For instance, they carefully tuned the viscosities of the inks to a similar level to avoid their mixture during extrusion. They also chose a tapered spinneret because the tapering channels speed up the fluid flow of the electrode inks at the exit, where the shear force is greatly enhanced. Hence, the resultant laminar flow between functional components guarantees seamless interfaces during extrusion. In addition, the strong shear force helps orient low-dimensional nanomaterials such as carbon nanotubes in the electrode inks. The highly aligned carbon nanotube network along the axial direction significantly reduces electrical resistance. Low electrical resistance for charge transport is vital to fully explore the energy-storage capabilities of the active materials in a battery.

Using this method, they produced 1,500 km of continuous FLIBs, more than three orders of magnitude longer fibres than previously reported. They also showed a proof-of-principle for roughly 10 m^2 of woven textile for smart tent applications, with a battery with an energy density of 550 mWh m^{-2}.

Apart from making FLIBs, the researchers can also use the method to produce other types of fibre batteries, such as Zn-MnO_2 batteries and sodium-ion batteries, by simply changing the ink materials.

"The method is straightforward, and the flexible textile battery obtained is stable, durable and safe," Liao and his colleagues wrote in their paper. "We envision a future where batteries can be worn like clothes and used to power a myriad of electronic devices."

References

He, J., Lu, C. and Jiang, H., *et al*. Scalable production of high-performing woven lithium-ion fibre batteries. *Nature* **597**, 57 (2021). doi: 10.1038/s41586-021-03772-0.
Liao, M., Wang, C. and Hong, Y., *et al*. Industrial scale production of fibre batteries by a solution-extrusion method. *Nature Nanotechnology* **17**, 372 (2022). doi: 10.1038/s41565-021-01062-4.

8th Quantum Walks on a Programmable Two-Dimensional 62-Qubit Superconducting Processor *Zuchongzhi*

Quantum walks, enabled by the quantum principles of superposition and entanglement, are the quantum mechanical counterpart of classical random walks. These walks can be a potent tool in quantum simulations, quantum search algorithms, and even universal quantum computing.

Published in *Science* in May 2021, a research team led by Pan Jian-Wei, Zhu Xiaobo, and Peng Cheng-Zhi from the University of Science and Technology of China (USTC) realized quantum walks on a programmable two-dimensional 62-qubits superconducting processor, which is named *Zuchongzhi* after the noted 5th century Chinese mathematician and astronomer.

The researchers designed and fabricated an 8-by-8 two-dimensional square superconducting qubit array composed of 62 functional quantum bits or qubits in this work. Unlike the classical bits, which can either be 0 or 1, qubits can simultaneously be 0 and 1. Using this device, they demonstrated high-fidelity single- and two-particle quantum walks.

Furthermore, with the high programmability of the quantum processor, they implemented a Mach-Zehnder interferometer where the quantum walker coherently traverses in two paths before interfering and exiting. By tuning the disorders on the evolution paths, they observed interference fringes with single and double walkers.

"Our work is a milestone in the field, bringing future larger scale quantum applications closer to realization on noisy intermediate-scale quantum processors," wrote the authors in the article.

The developed prototype of quantum processor *Zuchongzhi* contains the largest number of superconducting qubits in the world as of publication time. Using it, the researchers verify the high-precision quantum control capability over noisy medium-scale qubit systems, laying the foundation for upgrading the prototype and stepping into the realm of quantum supremacy.

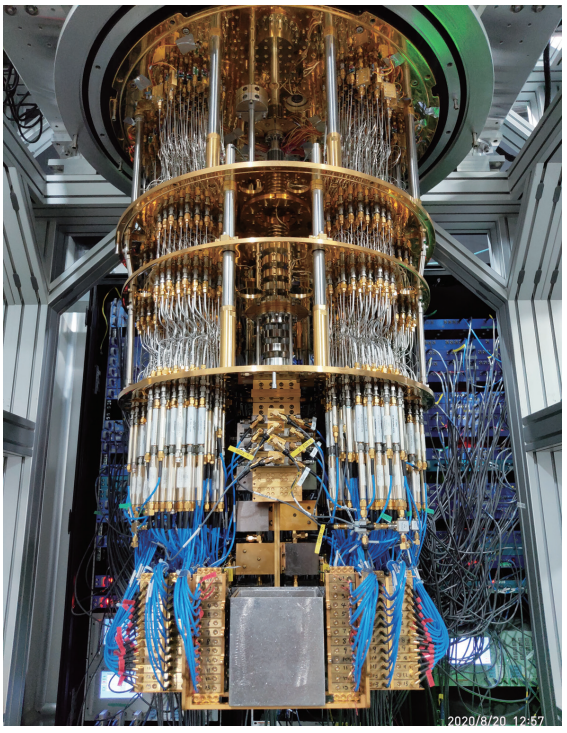

The new superconducting quantum processor *Zuchongzhi*. (Image by USTC)

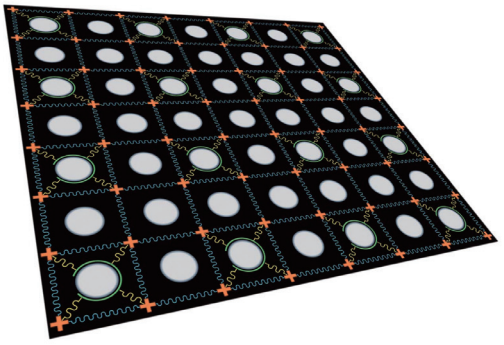

The schematic diagram of the 2D superconducting quantum processor. The orange crosses represent the quantum bits, or qubits, arranged in an 8-by-8 array. (Image by USTC)

Reference

Gong., M., Wang, S. and Zha, C., *et al*. Quantum walks on a programmable two-dimensional 62-qubit superconducting processor. *Science* **372**, 948 (2021). doi: 10.1126/science.abg7812.

9th Self-powered Soft Robot Braves the Mariana Trench

The ocean's deepest regions remain largely uncharted because of the extreme hydrostatic pressure. Given the tremendous resources and irrepressible human curiosity, we have developed various metal-shielded water-proof

robots or pressure compensation systems to withstand such tremendous crush power and completed many deep-sea explorations. However, these bulk designs still face all sorts of problems imposed by the distinct nature of the deep sea.

Nevertheless, the genius of nature enables a kingdom of organisms to populate in such depth. Inspired by the unique feature of the deep-sea snailfish, whose head bones are scattered and fused in soft tissues, LI Tiefeng *et al*. from Zhejiang University reported a robot made from soft materials that can operate in the Mariana Trench, the deepest part of the ocean.

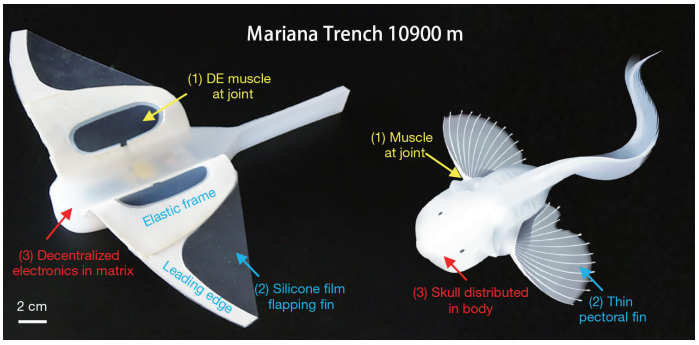

A soft robot inspired by a deep-sea snailfish with scattering bones within a soft body can brave the extreme hydrostatic pressure at a depth of 10900 m in the Mariana Trench. (Image by LI Tiefeng *et al.*)

The robot is designed to have a fish-like body and two flapping side fins. Like the snailfish's scattering bones, they implement electronics inside the soft body to improve their pressure resistance. When electric current flows into the artificial muscles, they deform. As a result, the attached fins flap, enabling the robot to swim.

This new design of scattering electronics with enhanced pressure resistance allows the robot to be actuated successfully in a field test in the Mariana Trench down to a depth of 10,900 m and to swim freely in the South China Sea at a depth of 3,224 m.

"Li and co-workers' research now pushes the boundaries of what can be achieved: the

replacement of rigid protective enclosures for electronic components by distributed electronics embedded in a soft material paves the way to a new generation of deep-sea explorers," as commented by two experts in the same issue.

One day, these soft robots may safely navigate coral reefs or the deepest seabed to collect delicate specimens without damaging them.

References

Li, G., Chen, X. and Zhou, F., *et al.* Self-powered soft robot in the Mariana Trench. *Nature* **591**, 66 (2021). doi: 10.1038/s41586-020-03153-z.
C. Laschi and M. Calisti. Soft robot reaches the deepest part of the ocean. *Nature* **591**, 35 (2021). doi: 10.1038/d41586-021-00489-y.

10th A Bird's Flyways and Migration Decoded

"How do migratory animals know where they're going?" is listed among the "125 Questions: What We Don't Know", a special issue released by *Science* in 2005. Migration is a ubiquitous feature of the animal kingdom, and is arguably studied most comprehensively in birds. Nearly two decades later, scientists can now provide a better answer to the mystery of a bird's flyways and migration evolution.

Writing in *Nature* in March 2021, a joint team led by ZHAN Xiangjiang from the Institute of Zoology (IOZ) of the Chinese Academy of Sciences confirmed how a combination of changing climate and genes drives evolution of migration in peregrine falcons (*Falco peregrinus*).

Using satellite transmitters attached to the birds' backs, they followed 56 peregrine falcons over several years to determine a total of 151 complete migration routes originating from 6 different populations that breed in the Eurasian Arctic, as shown in Fig.1. They also found that the western peregrine falcons are short-distance migrants while the east ones are long-distance migrants.

By resequencing the genomes of individuals from four different populations combined with ecological niche modeling, they identified distinct genetic clusters in which long-distance and short-distance migrants diverged during the Last Glacial Maximum (22,000 years ago). The divergence of the long-distance and short-distance populations coincides with changes in the availability of tundra habitat during breeding seasons in the arctic. They concluded that glacial cycles influence the falcons' migratory orientation and distance.

They also identified a signal of positive selection at the *ADCY8* locus in long-distance migrants, a gene previously linked to long-term memory. After looking into the regulatory mechanism of this gene, they suggested the long-term memory as the most likely selective agent for divergence in *ADCY8* among the peregrine populations, which makes sense considering that long-distance migration, compared to short-distance migration, requires stronger long-term memory.

With breeding and wintering grounds predicted to shift more than one degree poleward by 2070, the authors reckon that the short-distance peregrines may have a much shorter migration route, whereas long-distance migrants may have a longer route. As a result, the peregrines in western Eurasia may stop migrating altogether, and those in the eastern may face greater risks, as mortality is positively associated with migratory distance.

Their study demonstrates the value of an integrated approach that combines satellite telemetry, population and functional genomics, and modeling in gaining mechanistic insights into the evolution of migration routes and strategies, which will be valuable in informing future conservation efforts.

"Such insights enable the modelling of community dynamics across large time spans, including past and future scenarios," wrote two German scientists in the same *Nature* issue, who are not involved in this study.

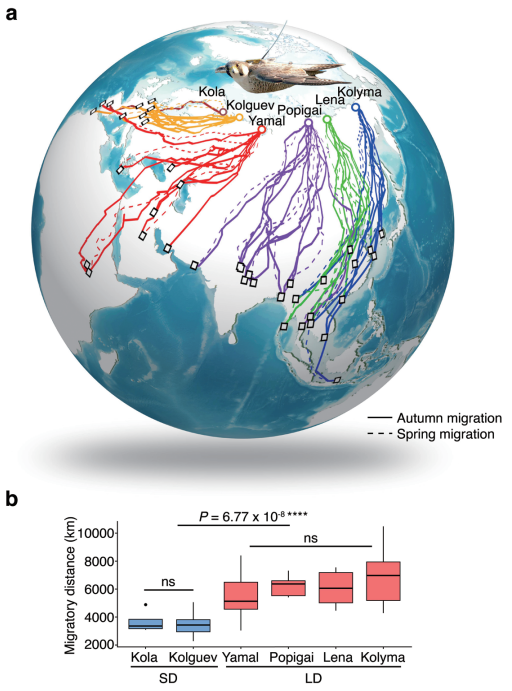

Fig.1 Five migration routes were identified from six Arctic-breeding populations of peregrine falcons using satellite tracking. Birds that breed in the western Eurasian Arctic (Kola and Kolguev) are short-distance (SD) migrants, whereas those breed in the eastern are long-distance migrants. (Image by IOZ)

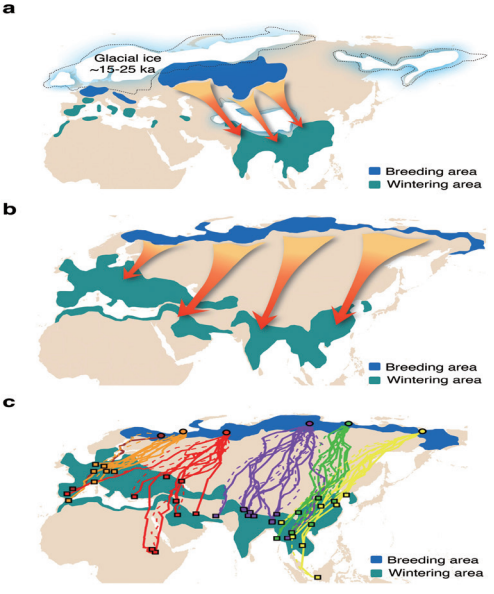

Fig.2 Species distributions predicted during the Last Glacial Maximum (a), middle of the Holocene (b) and present (c). (Image by IOZ)

References

Gu, Z., Pan, S. and Lin, Z., *et al*. Climate-driven flyway changes and memory-based long-distance migration. *Nature* **591**, 259 (2021). doi: 10.1038/s41586-021-03265-0.

S. Lisovski and M. Liedvogel, A bird's migration decoded. *Nature* **591**, 203 (2021). doi: 10.1038/d41586-021-00510-4.